WOOD RESEARCH doi.org/10.37763/wr.1336-4561/67.2.254267
e-ISSN 2729-8906
67(2): 2022 254-267 pp.

MODELLING A CLT SPECIMEN PROTECTED WITH GYPSUM EXPOSED TO PARAMETRIC FIRE CURVE HEAT FLUX

LINDA MAKOVICKA OSVALDOVA, PAULINA MAGDOLENOVA
UNIVERSITY OF ZILINA
SLOVAKIA

FRANK MARKERT
TECHNICAL UNIVERSITY OF DENMARK
DENMARK

SAMUEL L. ZELINKA
USDA FOREST SERVICE
UNITED STATES

LOUISE FREDERIKKE ENOKSEN
AFM RÅDGIVENDE INGENIØRER A/S
DENMARK

MALTHE KLINT
DBI - DANISH INSTITUTE OF FIRE AND SECURITY TECHNOLOGY
DENMARK

(RECEIVED OCTOBER 2021)

ABSTRACT

This paper models bench-scale experiments using computational fluid dynamics (CFD). The experiments measured the temperature profiles of fire-protected cross laminated timber (CLT) specimens exposed to parametric fire curve. The bench-scale experiment specimen is 250 x 250 mm and consists of a CLT panel 100 mm with three layers of gypsum plasterboard 15.5 mm as thermal and fire insulation The specimens were exposed to a heat flux generated by a heat-transfer rate inducing system (H-TRIS) device. Two numerical models were created in order to copy the experiment conditions, one by using basic modelling techniques and one using advanced method. Comparing the layer temperature values of the experiment and basic model, a great difference was found. The difference between experimental and model temperatures

increases the closer the analysed layer is to the heat source. The results show a good agreement between the model and the experiments, especially for the advanced numerical model.

KEYWORDS: CLT panel, gypsum-plaster board, H-TRIS, parametric fire curve, CFD model, fire protection.

INTRODUCTION

Presently, cross-laminated timber (CLT) is of great interest in the building industries. With numerous benefits of using CLT components in constructions, one drawback of the CLT is its combustibility (Emberley 2017). In most cases, to eliminate the fire safety drawbacks of wooden materials, fire protection needs to be applied. The fire retardant application approach has been investigated in recent years by scientific society (Makovická Osvaldová and Osvald 2013, Makovická Osvaldová et al. 2016, 2020, Eremina and Korolchenko 2020). Numerous studies to investigate how specifically CLT panels behave as a structural element in fire conditions have been performed. The studies analysed the CLT's response to fire with both unprotected CLT and fire protected CLT. Fire protection was applied using an active sprinkler system and passive fire protection using gypsum plasterboards (GPB) (Emberley 2017, McGregor 2014, Medina Hevia 2015, Kasymov et al. 2020, Solorzano et al. 2019).

Bench-scale tests are useful to conduct as a supplement to cope with the large-scale fire tests' disadvantages. Standard fire test methods are found to be small or intermediate scale. While cost-effective, fire engineers should be aware of the difficulty in extrapolating data from bench-scale type tests to large-scale events (Buc 2008).

According to (Babrauskas and Wickstrom 2016), standard bench-scale fire tests are generally conducted to cover one of these three purposes: *(1)* prediction of expected full-scale behaviour, *(2)* quality control assurance in manufacturing, and *(3)* guidance in product development. Experiments based on typical fire scenarios conducted with new materials before they are introduced into the market prove their safety before they cause a disaster (Williamson and Dembsey 1993). Numerical modelling is a way to bridge bench-scale and large-scale (Babrauskas 2016) and is becoming increasingly popular by fire engineers. The use of computer models for simulating enclosure fires has increased dramatically in recent years (Karlsson and Quintiere 2020). In addition, the availability of such tools can provide cost-effective alternatives by reducing the number of large-scale tests necessary to develop fire protection requirements or standards (Chaos et al. 2011).

Demonstrating the connection between numerical and experimental fire tests is crucial. Currently, advanced fire models can replace certain laboratory experiments (Babrauskas 1984). According to (Cabova et al. 2017), the first attempt to apply CFD modelling in standard testing was described in (Welch and Rubini 1997) using the computer code SOFIE (Simulation of fires in enclosures) to simulate fire-resistance wall furnace.

The mentioned studies combine and validate the CFD modelling with various types of small-scale laboratory fire tests, such as the fire test furnace (Thomas 2002, Piloto et al. 2009, Nassif et al. 2014, Karabas et al. 2016, Ing et al. 2017, Cayla et al. 2021) or the cone calorimetry

(McGregor 2014, Medina Hevia 2015, Kasymov et al. 2020). In the study (Hietaniemi et al. 2004), several models simulated small-scale cone calorimetry burning and large-scale single burning item (SBI) and bench-scale room corner tests. The study (Bytskov 2015) is focused on comparing the numerical simulation results to laboratory tests of various materials. Facade insulation materials were modelled in a scientific study by (Linteris et al. 2004) where both cone calorimetry, a façade fire and a small-scale flammability test methods were simulated and compared with experimental data.

This paper deals with the development of the FDS heat transfer model to simulate an H-TRIS (heat transfer rate inducing system) heat exposure to predict the heat transfer through multiple layers of a GPB protecting a CLT panel. This approach enables a simulation of thermal boundary conditions experienced by the materials or structures. Finally, the created model is validated by experimental work on this GPB/CLT system carried out at the Technical University of Denmark (DTU) (Hansen 2018, Enoksen and Klint 2018).

MATERIALS AND METHODS

As stated above, this paper continues prior DTU research using the H-TRIS test (Enoksen and Klint 2018). An advanced model of the H-TRIS is developed, enabling both the 1D and 3D heat transfer modelling. A GPB sub-model is also developed based on TGA (thermogravimetric analysis) measurements on the actual material. The model is validated using experimental data from (Enoksen and Klint 2018). The experiments measured the temperature profiles of fire-protected CLT specimens exposed to parametric fire curve.

The experiment specimen is 250 x 250 mm and consists of a CLT panel 100 mm with three layers of gypsum plasterboard 15.5 mm as thermal and fire insulation (Fig. 1).

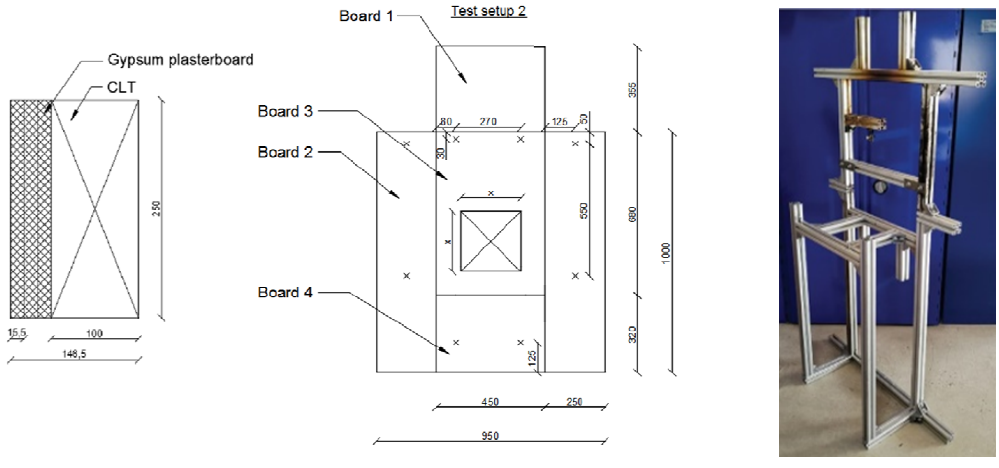

(a) (b) (c)

Fig. 1: (a) Experiment specimen cross-section, (b) noncombustible boards (NCBs) setup, (c) specimen setup aluminum frame.

The CLT panel used is LENO® CLT (Züblin Timber), spruce C24 with a density of 500 $kg \cdot m^{-3}$, thermal conductivity of 0.13 $W \cdot m^{-1} \cdot K^{-1}$ and specific heat capacity of 1600 $J \cdot kg^{-1} \cdot K^{-1}$.

The gypsum plasterboard (GPB) Knauf Ultra Board 15 U-1 was used with a density of 968 $kg \cdot m^{-3}$, the thermal conductivity of 0.25 $W \cdot m^{-1} \cdot K^{-1}$, and a specific heat capacity of 1000 $J \cdot kg^{-1} \cdot K^{-1}$. The non-exposed sides of the specimen were insulated with mineral wool Steico with a density of 50 $kg.m^{-3}$, thermal conductivity of 0.037 $W \cdot m^{-1} \cdot K^{-1}$, and a specific heat capacity of 840 $J \cdot kg^{-1} \cdot K^{-1}$. The specimen temperatures were measured with type K thermocouples from OMEGA that were centrically mounted into each layer of the GPB_CLT component 1 mm underneath the heat exposed surface.

As the source of heat in the experiment, the heat-transfer rate inducing system (H-TRIS) is used (Enoksen and Klint 2018, Maluk et al. 2019). The setup of the H-TRIS experiment is shown in Fig. 2.

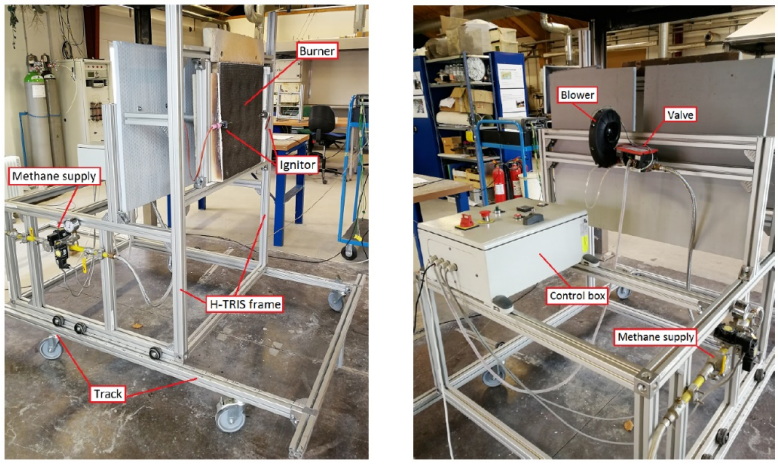

Fig. 2: (a) H-TRIS device front and side view, (b) back view.

The temperatures used in the experiment are mimicking a parametric fire curve for an apartment. The H-TRIS is not capable to reach the mean temperature higher than 536.9°C and because of that, the maximum temperature for the furnace was set to this temperature. The parametric fire curve shown in Fig. 3a was applied for the experiments. The fire curve was established by dividing the heating exposure into individual steps, as shown in Fig. 3b.

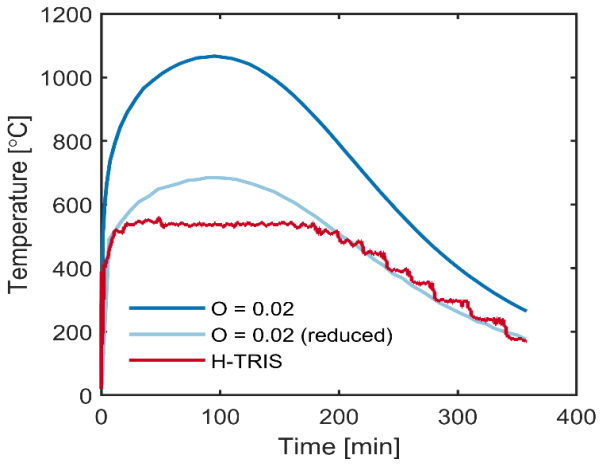

Step	Dist. to H-TRIS [m]	BI [%]	Duration [min]
1	0.15	49	5
2	0.15	72	5
3	0.13	60	10
4	0.13	75	10
5	0.13	85	15
6	0.13	100	95
7	0.13	85	20
8	0.13	75	20
9	0.13	60	20
10	0.15	68	20
11	0.15	50	20
12	0.20	61	20
13	0.20	40	20
14	0.30	68	30
15	0.30	10	30
16	0.55	54	60
17	1.00	10	200

Fig. 3: (a) Parametric fire curve for; (b) table of experiment time steps.

The specimen size 250 x 250 mm was chosen for the experiment because the specimen consisted of multiple GPBs and the CLT panel, which would lead to the specimen thickness greater than the width for a size of 150 x 150 mm. Additionally, the specimen size 250 x 250 mm was optimal for the experiment because of the down-scale ratios of the GPBs and CLT panel to acquire a quite uniform heat exposure distribution. The most uniform heat exposure would of course be within a smaller 150 x 150 mm specimen size. The total heat exposure time of the conducted experiment was 143 min (Enoksen and Klint 2018).

Numerical model

According to the experiment the numerical FDS model of the heat transfer was created according to official software user guide (McGrattan and Forney 2004). The FDS represents a computational fluid dynamics (CFD) model and numerically solves a form of the Navier-Stokes equations appropriate for low-speed, thermally-driven flow, emphasising smoke and heat transport from fires (Maluk et al. 2019).

Two model scenarios were created to focus on the heat transfer inside the specimen layers and the temperature profile analysis. These two scenarios differ by using basic (Scenario 1) and advanced (Scenario 2) modelling techniques, briefly summarised in Tab. 1. These scenarios should not only confirm/disprove the numerical model ability to reproduce and replace this type of bench-scale experiment but also provide the basis for the software development analysis. Such analysis will show if using advanced modelling tools of the FDS software impacts the simulation analysis and brings more satisfying results comparing to the basic scenario. Both scenarios ran on high-performance computing, HPC, cluster with Linux OS at DTU in the newest FDS version 6.7.5.

Tab. 1: Modelling techniques applied in Scenario 1 and Scenario 2.

Modelling approach	Basic (Scenario 1)	Advanced (Scenario 2)
3D heat transfer	-	✓
3D pyrolysis	-	✓
TGA data input	-	✓ (GPB)
FDS TGA analysis	-	✓ (GPB)
Temperature measuring device (&DEVC) type	inside_wall_ temperature	temperature and thermocouple
GPB absorption coefficient	50 000 (software default)	12 990 (calculated for GPB)
Specimen mesh grid size	0.020x0.025x0.025	0.005x0.005x0.005

As the created scenarios do not approach flashover conditions, it is appropriate for the FDS model to set up for both scenarios the commands “STRATIFICATION=.FALSE.” and “SUPPRESSION=.FALSE.” to reduce the computational time (McGrattan and Forney 2004). To secure the heat transfer between solids (the H-TRIS radiation panel and the specimen) the command “RADIATION=.TRUE.” was added. The time step recording the measuring device outputs was set to 1 s. In both scenarios, only half of the experiment setup was modelled using the MIRROR function. The symmetry axis was set alongside the vertical axis in the middle of the radiation panel and specimen. By applying this function, the computing time was reduced without any effect on the results. For this reason, only half of the modelled area is shown in the

following figures. Instead of a 500 x 500 mm radiation panel, only 250 x 500 mm is shown and accordingly for the specimen and the surrounding NCBs. Total simulation time was set up to 7200 s in both scenarios. The distance between the radiation panel and specimen surface is in both scenarios set to 0.130 m during the whole simulation time to reproduce the experimental conditions (Fig. 3b), but ignoring the first 10 min when the distance was 0.150 m.

There are no differences between Scenario 1 and 2 in the H-TRIS panel modelling approach. However, starting the modelling process by applying the experimental heat flux evenly on the whole radiation panel brought a much more homogeneous heat flux on the specimen surface than the heat flux measured during the H-TRIS calibration. The model was afterwards modified to increase the heat flux towards the radiation panel centre as it is supplied with methane and air from the centre and the panel surface is not completely flat – the panel centre is slightly closer to the specimen surface than the panel edges. The modification is based on dividing the panel area into five frames (rings), each 50 mm thick. Different heat flux is applied on each of these frames, varying from 118 $kW \cdot m^{-2}$ to 165 $kW \cdot m^{-2}$ (Fig. 4).

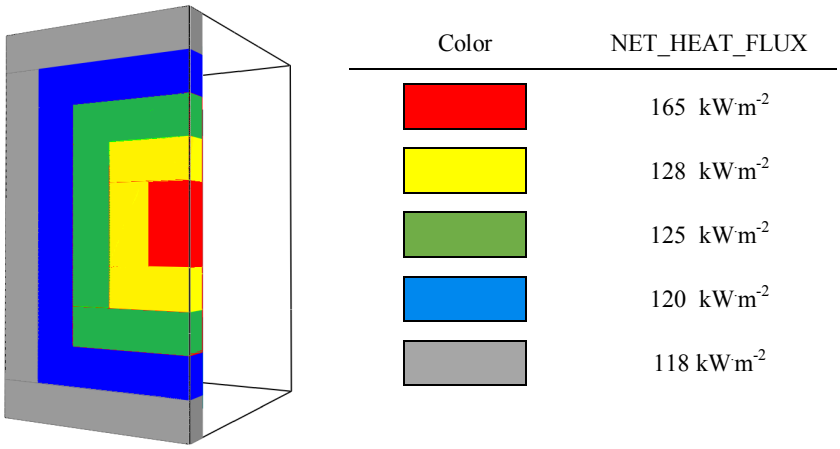

Fig. 4: H-TRIS panel model.

The H-TRIS panel has an individual mesh in the model with a cell size of 30 × 25 × 25 mm for both scenarios. Parts of the H-TRIS frames were modelled as obstacles with the associated surface. For the H-TRIS, five surfaces have been created with different net heat fluxes and a uniform time-dependent heat release rate according to the measured heat flux data at the specimen centre.

Numerical model – Scenario 1

In Scenario 1, the basic scenario, the specimen and NCBs were modelled in one mesh with the cell size 20 × 25 × 25 mm. In total, four materials are defined to model the specimen – CLT, GPB, NCB and mineral wool. For all materials, density, thermal conductivity and specific heat capacity were defined with the values mentioned above in the experimental description. However, all of these values were determined at standard room temperature (20°C), and they are usually a function of temperature. Because of that, a ramp function is activated for the specific heat capacity and thermal conductivity to define their temperature dependence. In FDS, it is not

possible to define density as a temperature-dependent parameter. The CLT thermal properties are considered to be the same as for spruce wood. Therefore, values provided by a study by (Jones 2001) are chosen as input values for the model. TGA results of the GPB confirmed that the chosen GPB type does not contain any $CaCO_3$, which allows us to use data for the temperature-dependent parameters in the model. For NCB, only the conductivity development when heated up is available. All other parameters are defined with the values at standard room temperature.

Numerical model – Scenario 2

Scenario 2 was created with a more advanced approach to obtain more precise results. The difference between the advanced approach and Scenario 1 is the application of a 3D solid heat transfer sub-model on the specimen materials, which is still under development and currently only available in a beta version implemented in the FDS code. The 3D solid heat transfer (further referred to as HT3D) method in FDS is a conduction model that accounts for lateral heat transfer within a solid (McGrattan and Forney 2004). By default, FDS is capable only of calculating one-dimensional heat transfers through objects. The 3D heat transfer method brings a more advanced way of a solid material definition in fire models. As it could provide more precise outputs of a solid structure's thermal behaviour, it represents the main aim of this paper to evaluate its performance.

For the HT3D, every layer of the specimen must be specified as an individual obstacle (&OBST) and should be at least one mesh cell thick. As mentioned above, the specimen has three layers of 15.5 mm thick GPB which would lead to a 0.5 mm size numerical grid cell. The computing time is reduced by simplifying the thickness of GPBs to 15 mm, which allowed us to create an individual mesh for the specimen with a 5 mm grid cell. Creating a 15 mm grid cell would considerably speed up the computing time. However, such a mesh would not be compatible with H-TRIS mesh with 25 mm and is therefore adjusted to the particular H-TRIS panels dimensions.

Because of extremely long computing time (approximately 1400 s of simulation for 24 hours of computing), efforts to reduce the computing time were undertaken. At first, the specimen part of the model was divided into four meshes to separate the specimen areas, which requires a very small grid size of 5 × 5 × 5 mm. With a bigger grid size of 20 × 25 × 25 mm, three meshes were created to surround the specimen from above, under, and alongside with obstacles representing rock wool specimen insulation. There was also an effort to eliminate these three meshes by replacing them with surrounding surfaces of the specimen using the SURF_IDS command. Still, it is not possible to use this command by activated HT3D. The final visualisation of the modelled space is shown in Fig. 5, with the colour distinction of particular surfaces assigned to created obstacles.

The GPBs were modelled as one-layered material. However, besides gypsum, they consist of two layers of paper on the surface as an adhesive material. In terms of combustion, adding these layers would make the model more advanced as both are considered to burn. Adding the possibility of the paper layer combustion would increase the heat released, which would heat the GPB. However, as mentioned above, applying HT3D requires all material layers to be

specified as individual obstacles and each obstacle to be at least one mesh cell thick. Therefore, it is not possible to model the paper layers on GPB panel. However, other values for accurate GPB material characteristics were obtained at different sources and applied as summarised:

Emissivity ε for GPB was set to 0.9 (same as in the Scenario 1) which is the value for both paper layer and gypsum plaster, according to (Emissivity coefficients materials 2020, available online: https://www.engineeringtoolbox.com/emissivity-coefficients-d_447.html).

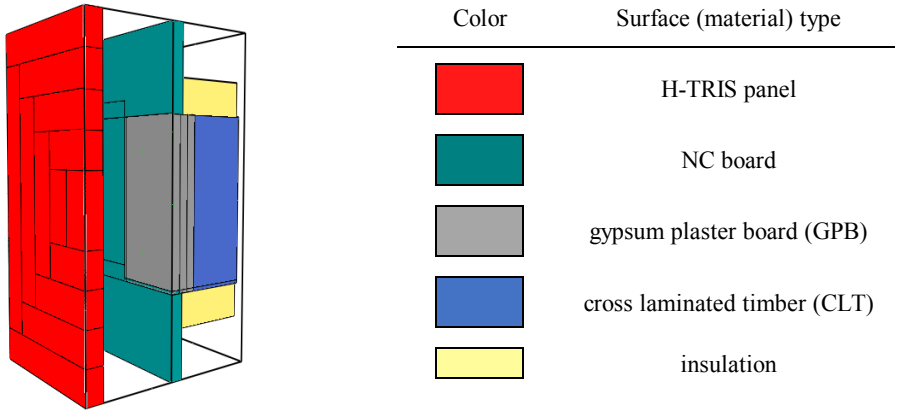

Fig. 5: Modelled space for numerical simulation.

Thermal absorption coefficient β_n for GPB was applied (otherwise, the default FDS value is 50 000 in the simple model) with the value of 12 990 m^{-1} based on a calculation from (Thermal absorption coefficient 2020, available online: http://scienceworld.wolfram.com/physics/ThermalAbsorptionCoefficient.html):

$$\beta_n = \frac{n.\rho.c_p}{2.k} \tag{1}$$

where: n - the number of moles → 5.271 mol based on the molecular weight of gypsum plaster (Gypsum mineral data 2020, http://webmineral.com/data/Gypsum.shtml#.Xhxz1iM1WUl), ρ - material density → 968 $kg.m^{-3}$, c_p - heat capacity → 1.273 $J.K^{-1}$ determined for GPB by 20°C according to (Robie et al. 1989), k - thermal conductivity → 0.25 for GPB by 20°C.

Most importantly, in terms of advanced modelling, characteristics such as latent heat and heat of reaction were applied based on the TGA measurement results of pure gypsum carried out at DTU (Enoksen and Klint 2018). According to the FDS user guide instructions and one of the FDS developer's work, measurement results were applied, which was focused on the TGA analysis in the FDS software (Matala et al. 2008). After the GPB material characteristics definition, the TGA analysis in the FDS was conducted, and outputs were compared to the real TGA measurement results. Usually, the comparison of TGA measurement and TGA numerical analysis is presented by two charts: mass to temperature and mass loss rate (MLR) to temperature. The more these curves match, the more precise are inputs for further FDS

calculations. Fig. 6 shows these two charts for GPB, as results of carried out TGA measurement and numerical analysis, which are considered sufficiently compatible.

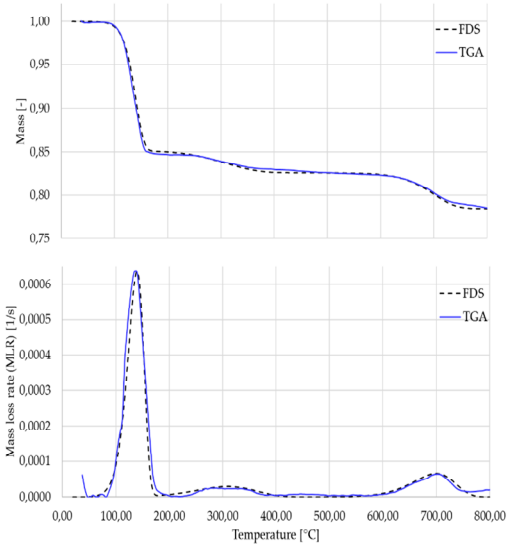

Fig. 6: TGA analysis in FDS and TGA measurement results comparison.

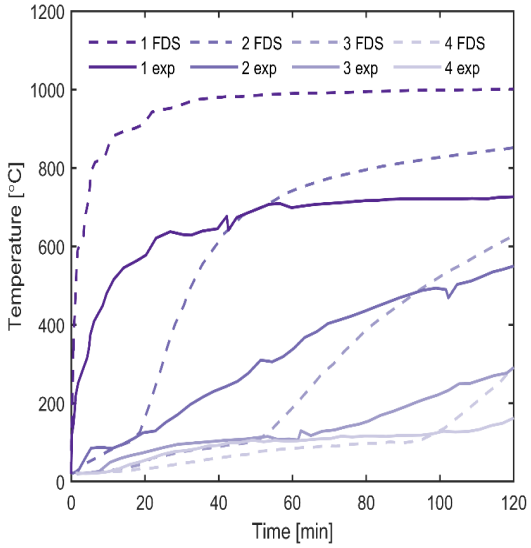

Fig. 7: Scenario 1 and experimental results.

RESULTS AND DISCUSSION

The solid lines in Fig. 7 show the temperature development of 1 mm underneath each specimen layer during the whole experiment time. As mentioned above, in the model description, numerical model temperatures in the specimen layers are recorded by measuring devices (&DEVC) with different quantities specified. In case of the Scenario 1, the devices are specified with 'INSIDE_WALL_TEMPERATURE' quantity, and its outputs are shown in Fig. 7 (dashed line curves) together with the experimental results for better comparison.

Scenario 1, presented in Fig. 7, shows that the basic model of the heat transfer responds to the sample layering. That is acknowledged not only by significantly different temperature values of each GPB and CLT layer but also by the sharper increase of each layer temperature curve. However, comparing the layer temperature values of the experiment and basic model, we can see a great difference. The difference between experimental and model temperatures increases the closer the analysed layer is to the heat source. We can also see that the temperature curves of the 2nd, 3rd and 4th material layer show a match in the simulation beginning and starts to differ significantly the later the layer is further from the heat source. In Scenario 2, two types of devices are used - 'TEMPERATURE' and 'THERMOCOUPLE'. Its results are shown in Fig. 8 together with the experimental data for better comparison.

The results of the 'TEMPERATURE' device quantity (Fig. 8a) show a similar course comparing to Scenario 1 (Fig. 7) for GPB layer 1 and 2. However, the difference between experimental and numerical values is moderately reduced. The temperature data for layers 3 and 4 show better matches and the difference of the experimental and numerical value is reduced significantly compared to Scenario 1. The obtained temperature results measured with

'THERMOCOUPLE' device quantity (Fig. 8b) show significant difference reduction comparing to Scenario 1 and 'TEMPERATURE' device quantity. The temperature value match of experiment and numerical model results is achieved in all material layers on a satisfying level. That shows that the new FDS 3D heat transfer method applied in Scenario 2 offers a great accuracy rate. Code used on all scenarios 1 and 2 for FDS simulation is part of Technical University of Denmark research (Experiments and model development to predict temperature profiles in fire protected CLT elements exposed to parametric fire curves) using the H-TRIS test (Enoksen and Klint 2018).

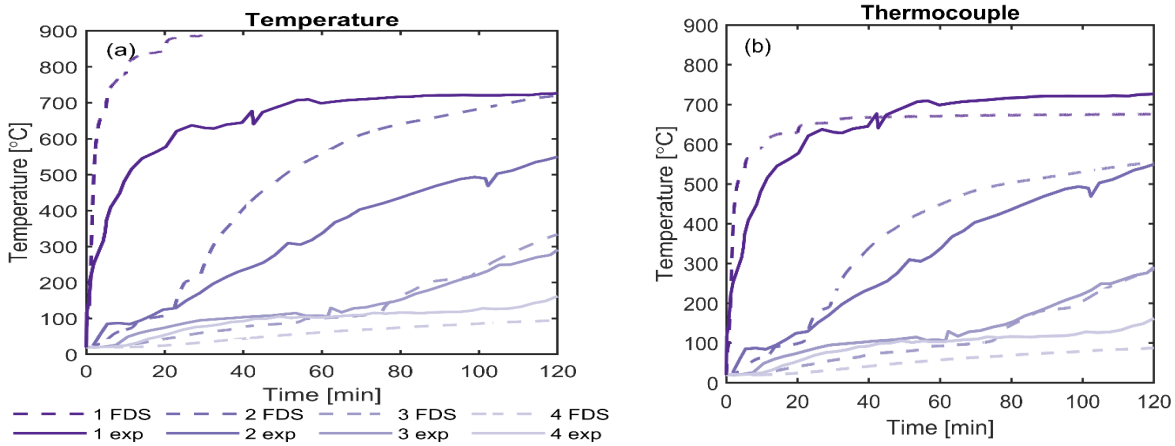

Fig. 8: Scenario 2 and experiment results; (a) device quantity 'TEMPERATURE'; (b) device quantity 'THERMOCOUPLE'.

According to the obtained results, we can say that the standard 1D heat transfer method applied in the FDS (Scenario 1) corresponds with the sample material layering (Fig. 7), which proves the partial model ability to reproduce conducted experiment. However, comparing to experimental data, the material temperature difference is significant. Consequently, the basic model cannot be used as a validation study for further bench-scale heat transfer CFD modelling.

The 3D heat transfer method, currently available in the FDS beta version, represents satisfying results by properly chosen measuring devices quantity. As the results show (Fig. 8), the device quantity 'THERMOCOUPLE' should be applied for accurate output data. As thermocouples were also used to measure the temperature during the experiment, these results show the FDS model ability to respond to the temperature measuring method type sensitively. The results obtained in Scenario 2 with thermocouples (Fig. 8b) support the progress of numerical model development applied in the FDS software and its wider ability to reproduce bench-scale heat transfer experiments. The deviation between experimental and 3D heat transfer numerical data in Fig. 8b is largely caused by the remaining numerical model inaccuracy, as the model cannot intercept the real conditions for 100%. However, to a partial extent, the deviation could also be caused by measurement inaccuracies during the experiment supported by vacillating temperature development in certain parts of the temperature curves.

Despite the result deviation, the 3D heat transfer model (Fig. 8) can be considered accurate and be presented as validation for further numerical model application in the field of heat transfer.

CONCLUSIONS

The results confirm agreement between the FDS model and experimental results. According to the results, numerical models could be used instead of, or together with H-TRIS measurements. Advanced modelling techniques are essential to obtaining more precise outputs as results show that the Scenario 2 results are significantly closer to the experiment than the Scenario 1 results. Although the results from created Scenario 2 bring satisfying match with the bench-scale fire test data, they are not a perfect match. The gap between numerical and experimental outputs covers software imperfections, deviations and modelling simplifications that cannot be solved yet.

The analysis of the FDS numerical models utilising the 1D and 3D heat transfer technology was carried out by comparing the obtained data with experimental results. The analysed sample consists of the CLT panel, which is fire protected by 3 layers of the GPB and is exposed to the H-TRIS apparatus's parametric fire curve heat flux. The compared temperatures are measured at the surface of each sample layer in both experiment and numerical models.

Based on the obtained numerical results, we can say that numerical model development is essential. The study accentuates the heat transfer numerical method progress in the software FDS which implies the 3D heat transfer, currently in beta version. The acquired results show that the 3D heat transfer method sensitively responds to the entered input data. Consequently, applying newly developed features such as 3D solid heat transfer and 3D pyrolysis is reasonable to make the models more accurate and use enhanced material characteristics obtained by custom measurements, such as TGA in this instance.

Based on the study results, utilising the FDS numerical models based on the CFD method and implying the 3D heat transfer method is an appropriate way to reduce or eliminate bench-scale heat transfer experiments. Although the scenario definition and computing process may seem time-consuming, the model offers a great ability to vary needed input data according to the research. By using computing cluster for parallel jobs, a lot of time, money and material can be saved by using numerical models instead of experiments if the conditions are appropriate.

ACKNOWLEDGEMENT

This research was financially supported of the project KEGA 020STU – 4/2021 Building an innovative teaching laboratory for practical and dynamic education of students in the field of occupational safety and health.

REFERENCES

1. Babrauskas, V., 1984: Bench-scale methods for prediction of full-scale fire behavior of furnishings and wall linings. Society of Fire Protection Engineers, Boston, MA.
2. Babrauskas, V., 2016: The role of bench-scale test data in assessing real-scale fire toxicity. US Government Printing Office.
3. Babrauskas, V., Wickstrom, U., 1989: The rational development of bench-scale fire tests for full-scale fire prediction. Fire Safety Science. Pp 813–822.
4. Buc, E.C., 2008: Fire testing and fire reality: What do fire tests really tell us about materials? Fire & Building Safety in the Single European Market. Pp 61-69.
5. Bytskov, G., 2015: Numerical simulation of sire performance and test conditions for façade insulation materials. Master's Thesis, Aalto University, Espoo, 113 pp.
6. Cabová, K., Benysek, M., Liskova, N., Wald, F.A.E., 2017: Numerical simulation of fire-resistance test. Proceedings of the International Conference of Applications of Structural Fire Engineering (ASFE 2017). Manchester, United Kingdom. Pp 171-177.
7. Cayla, F., Leborgne, H., Joyeux, D., 2011: Application of a virtual resistance furnace: fire resistance test simulation of a plasterboard membrane. Proceedings of ASFE Conference 2011, Prague. Pp 343–348.
8. Chaos, M., Khan, M.M., Krishnamoorthy, N., de Ris, J.L.; Dorofeev, S.B., 2011: Evaluation of optimisation schemes and determination of solid fuel properties for CFD fire models using bench-scale pyrolysis tests. Proceedings of the Combustion Institute. Pp 2599–2606.
9. Emberley, R., 2017: Fundamentals for the fire design of cross laminated timber buildings. The University of Queensland, 117 pp.
10. Enoksen, L.F., Klint, M., 2018: Experiments and model development to predict temperature profiles in fire protected CLT elements exposed to parametric fire curves. Technical University of Denmark (DTU).
11. Eremina, T., Korolchenko, D., 2020: Fire protection of building constructions with the use of fire-retardant intumescent compositions. Buildings 10(10): 185.
12. Hansen, N.K., 2018: Fire protection systems for combustible constructions in parametric fires. Technical University of Denmark (DTU).
13. Hietaniemi, J., Hostikka, S., Vaari, J., Building, V., 2004: FDS simulation of fire spread – comparison of model results with experimental data. VTT report, 55 pp.
14. Ing, A.S., Martel, D.S., Lynch, K.N., Sharp, T.J., 2017: Design of small-scale furnace for fire resistance testing of building construction materials.
15. Jones, B.H., 2001: Performance of gypsum plasterboard assemblies exposed to real building fires. University of Canterbury, 174 pp.
16. Karabas, O., Kaplan, Ö., Yigit Suleyman, K., Gür, M., 2016: Numerical investigation of temperature distribution in a fire resistance test furnace. 4th International Symposium on Innovative Technologies in Engineering and Science (ISITES2016). Antalya, Turkey.
17. Karlsson, B., Quintiere, J.G., 2000: Enclosure fire dynamics; environmental and energy engineering series. CRC Press: Boca Raton, FL.

18. Kasymov, D., Agafontsev, M., Perminov, V., Martynov, P., Reyno, V., Loboda, E., 2020: Experimental investigation of the effect of heat flux on the fire behavior of engineered wood samples. Fire 3,4: 61.
19. Linteris, G., Gewuerz, L., Mcgrattan, K., Forney, G., 2004: Modeling solid sample burning with FDS. National Institute of Standards and Technology 7178 (2004): 36.
20. Makovická Osvaldová, L., Gašpercová, S., Mitrenga, P., Osvald, A., 2016: The influence of density of test specimens on the quality assessment of retarding effects of fire retardants. Wood Research 61(1): 35–42.
21. Makovická Osvaldová, L., Kadlicova, P., Rychly, J., 2020: Fire characteristics of selected tropical woods without and with fire retardant. Coatings 10(6): 527.
22. Makovická Osvaldová, L., Osvald, A., 2013: Flame retardation of wood. AMR 690: 1331–1334.
23. Maluk, C., 2014: Development and application of a novel test method for studying the fire behaviour of CFRP prestressed concrete structural elements. The University of Edinburgh, 506 pp.
24. Maluk, C., Bisby, L., Krajcovic, M., Torero, J.L., 2019: A heat-transfer rate inducing system (H-TRIS) test method. Fire Safety Journal 105: 307–319.
25. Matala, A., Hostikka, S., Mangs, J., 2008: Estimation of pyrolysis model parameters for solid materials using thermogravimetric data. Fire Safety Science 9: 1213–1223.
26. McGrattan, K.B., Forney, G.P., 2004: Fire dynamics simulator (version 6). User's guide. National institute of standards and technology. Gaithersburg, MD, NIST SP.
27. McGregor, C.J., 2014: Contribution of cross laminated timber panels to room fires. PhD. thesis, Carleton university, 186 pp.
28. Medina Hevia, A.R., 2015: Fire resistance of partially protected cross-laminated timber rooms. Thesis, Carleton University: Ottawa, Ontario, 199 pp.
29. Nassif, A.Y., Yoshitake, I., Allam, A., 2014: Full-scale fire testing and numerical modelling of the transient thermo-mechanical behaviour of steel-stud gypsum board partition walls. Construction and Building Materials 59: 51-61.
30. Piloto, P.A.G., Mesquita, L.M.R., Pereira, A., 2009: Thermal analysis in fire-resistance furnace. Proceedings of Advanced Research Workshop Fire Protection and Life Safety in Buildings and Transportation Systems, GIDAI: Santander, Spain. Pp 103-111.
31. Robie, R.A., Russell-Robinson, S., Hemingway, B.S., 1989: Heat capacities and entropies from 8 to 1000 K of langbeinite (K2Mg2(SO4)3), anhydrite (CaSO4) and of gypsum ($CaSO_4 \cdot 2H_2O$). Thermochimica Acta 139: 67–81.
32. Solorzano, J.A.P., Moinuddin, K.A.M., Tretsiakova-McNally, S., Joseph, P., 2019: A study of the thermal degradation and combustion characteristics of some materials commonly used in the construction sector. Polymers 11(11): 1833.
33. Thomas, G., 2002: Thermal properties of gypsum plasterboard at high temperatures. Fire Materials 26: 37-45.
34. Welch, S., Rubini, P., 1997: Three-dimensional simulation of a fire-resistance furnace. Proceedings of the fifth international symposium Fire safety science. Fire Safety Science, Melbourne, Australia. Pp 1009–1020.

35. Williamson, R.B., Dembsey, N.A., 1993: Advances in assessment methods for fire safety. Fire Safety Journal 20(1): 15–38.

LINDA MAKOVICKA OSVALDOVA*, PAULINA MAGDOLENOVA
UNIVERSITY OF ZILINA
FACULTY OF SECURITY ENGINEERING, DEPARTMENT OF FIRE ENGINEERING
UNIVERZITNA 1
010 26 ZILINA
SLOVAKIA
*Corresponding author: linda.makovicka@uniza.sk

FRANK MARKERT
TECHNICAL UNIVERSITY OF DENMARK
FACULTY OF CIVIL ENGINEERING, DEPARTMENT OF CIVIL ENGINEERING
BROVEJ, 118, 246
2800 KGS. LYNGBY
DENMARK

SAMUEL L. ZELINKA
USDA FOREST SERVICE
FOREST PRODUCTS LABORATORY, BUILDING AND FIRE SCIENCES
ONE GIFFORD PINCHOT DRIVE
WI 53726 MADISON
UNITED STATES

LOUISE FREDERIKKE ENOKSEN
AFM RÅDGIVENDE INGENIØRER A/S
EGEDAL, HOVEDSTADEN,
DENMARK

MALTHE KLINT
DBI - DANISH INSTITUTE OF FIRE AND SECURITY TECHNOLOGY
JERNHOLMEN 12
2650 HVIDOVRE
DENMARK